Tanaka et al, Supplementary Fig. 1

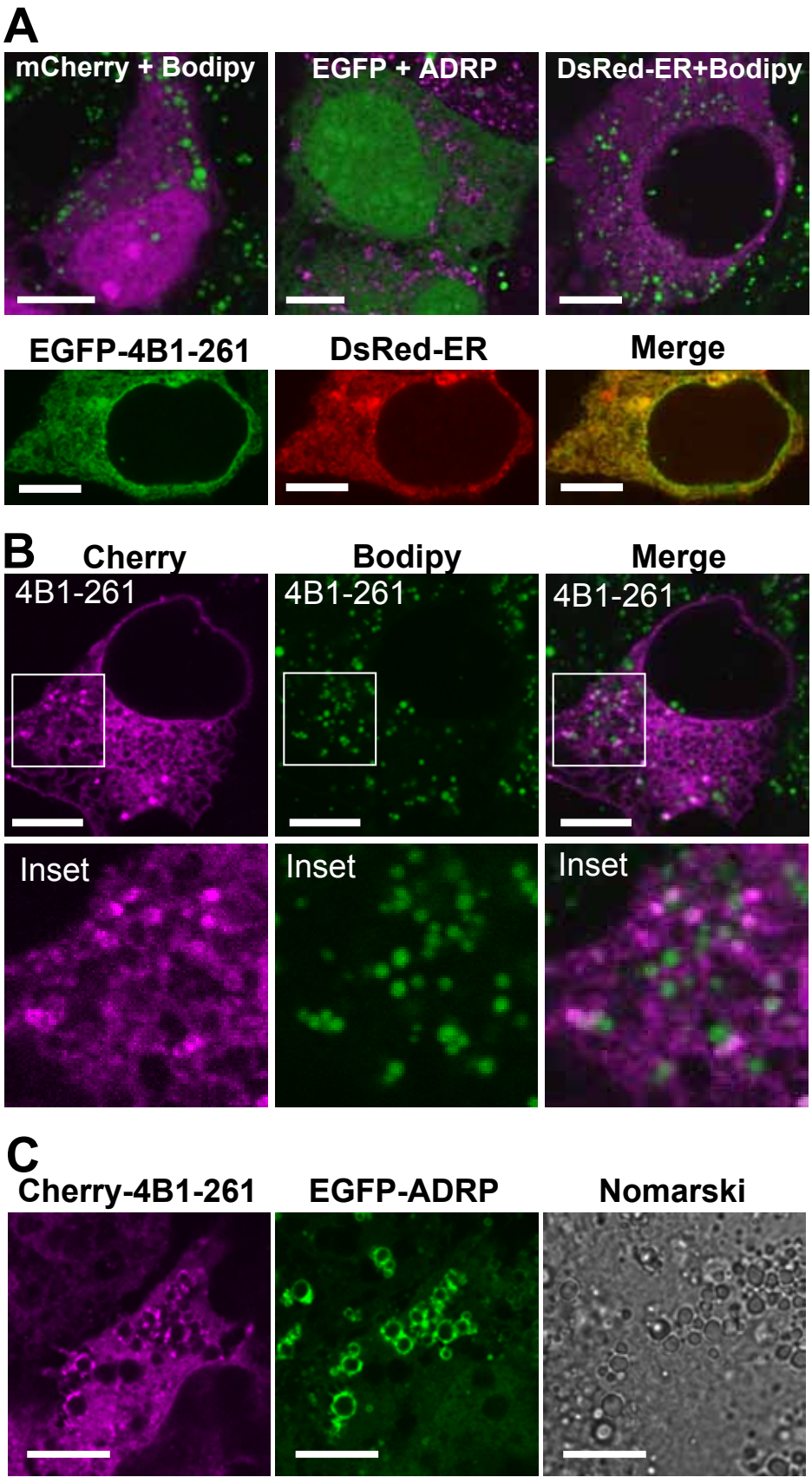

Tanaka et al, Supplementary Fig. 2

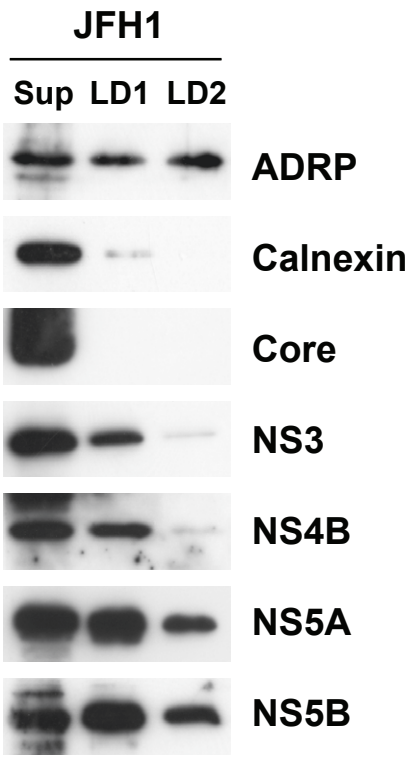

Tanaka et al, Supplementary Fig. 3

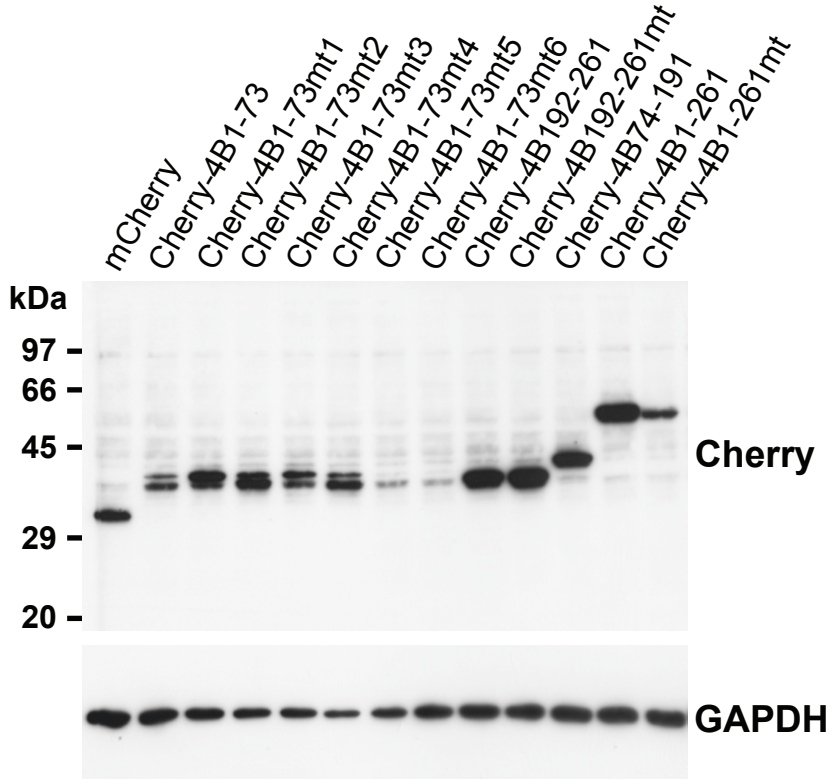

Tanaka et al, Supplementary Fig. 4

Subtype	Accession number	Amino acid									
		43	46	50	57	61	64	242	246	249	253
1a	EF407412	W	L	W	F	I	L	V	L	L	I
1b	AB191333	W	L	W	F	I	L	I	L	L	I
1c	D14853	W	L	W	F	I	L	V	L	L	I
2a	AF238481	W	V	W	F	I	L	I	L	L	I
2b	AAF59945	W	L	W	F	I	L	I	L	L	I
2c	Q68749	W	L	W	F	I	L	I	L	L	I
2i	DQ155561	W	L	W	F	I	L	I	L	L	I
2k	AB031663	W	L	W	F	I	L	I	L	L	I
3a	Q81495	W	L	W	F	I	L	V	L	L	I
3b	D49374	W	A	W	F	I	L	V	L	L	I
3k	D63821	W	L	W	F	I	L	V	L	L	I
4a	Y11604	F	L	W	F	I	L	V	L	L	I
5a	Y13184	W	A	W	F	I	L	V	L	L	I
6a	Y12083	W	V	W	F	I	L	I	L	L	V
6b	D84262	W	V	W	F	I	L	I	L	L	I
6c	EF424629	W	L	W	F	I	L	I	L	L	I
6d	D84263	W	L	W	F	V	L	I	L	L	I
6e	DQ314805	W	L	W	F	I	L	I	L	L	I
6f	DQ835760	W	V	W	F	I	L	I	L	L	I
6g	D63822	W	L	W	F	I	L	I	L	L	I
6h	D84265	W	L	W	F	I	L	V	L	L	I
6i	DQ835762	W	L	W	F	I	L	V	L	L	I
6j	DQ835761	W	L	W	F	I	L	V	L	L	I
6k	D84264	W	L	W	F	I	L	V	L	L	I
6l	EF424628	W	L	W	F	I	L	I	L	L	V
6m	DQ835763	W	L	W	F	I	L	I	L	L	I
6n	AY878652	W	L	W	F	I	L	I	L	L	I
6o	EF424627	W	L	W	F	I	L	I	P	L	I
6p	DQ155560	W	L	W	F	I	L	I	L	L	I
6q	EF424625	W	L	W	F	I	L	I	L	L	I
6t	EF632069	W	V	W	F	V	L	I	L	L	I
7a	EF108306	F	V	W	F	I	L	I	L	V	A

Tanaka et al, Supplementary Fig. 5

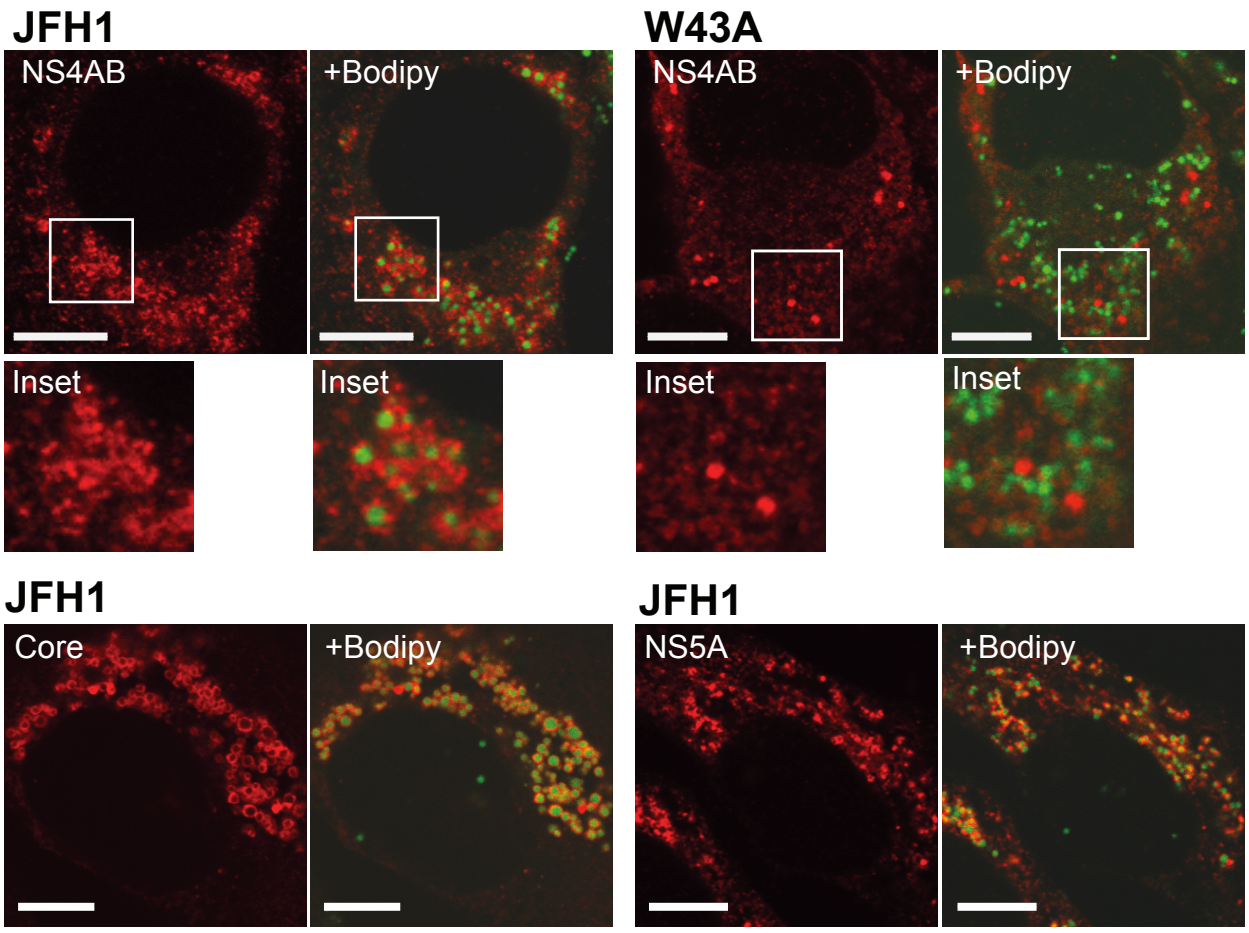

Tanaka et al, Supplementary Fig. 6

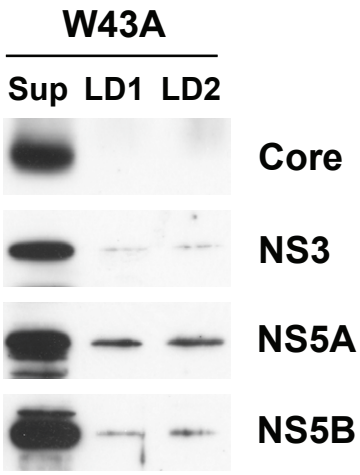

Supplementary Fig. 1. Comparative localization of native mCherry, native EGFP, and Cherry-4B1–261. (A) Top. Left, localization of mCherry. Center, localization of EGFP. ADRP was stained with anti-ADRP antibody. Right, localization of ER marker DsRed-ER. Bottom. Distribution of EGFP-4B1–261 and DsRed-ER. Oc cells were cotransfected with the plasmids for 24 h. Scale bars, 10 μm. (B) Localization of Cherry-4B1–261 to LDs. The image was obtained as in Fig. 1A, but from an independent experiment. Scale bars, 10 μm. (C) Colocalization of Cherry-4B1–261 with EGFP-ADRP. The same image as shown in Fig 1B right end panel. Images of each color channel and of Nomarski differential interference contrast are shown. Scale bars, 10 μm.

Supplementary Fig. 2. Localization of HCV antigens to LD preparations obtained from JFH1-RNA-transfected cells. LDs were prepared as in Fig. 2 (right) from Oc cells transfected with JFH1 RNA. The fractions were analyzed by immunoblotting.

Supplementary Fig. 3. Expression of various Cherry-4B constructs in Oc cells. Indicated constructs were transfected into Oc cells in 24-well plates for 24 h. One tenth (or 6/100) of the cells in each well were subjected to immunoblot analysis visualized with anti-mCherry antibody (Top) (or anti-GAPDH antibody; bottom).

Supplementary Fig. 4. Hydrophobic amino acid residues critical for LD targeting are highly conserved among various HCV subtypes. Ten amino acid residues (43W, 46L, 50W, 57F, 61I, 64L, 242I, 246L, 249L, and 253I) were aligned for various subtypes of HCV. For each subtype, the representative sequence, for which the full-length genome sequence was confirmed, was randomly chosen (except for AB191333, HCV-O).

Supplementary Fig. 5 Localization of HCV antigens in cells transfected with JFH1 or W43A RNA. Scale bars, 10 μm. Images of top panel were obtained from the same experiments as in Fig. 5B but with different cells.

Supplementary Fig. 6. Localization of HCV antigens to LD preparations obtained from W43A-RNA-transfected cells. LDs were prepared as in Fig. 2 (right). The LD preparation samples used in Fig. 5C were analyzed.